Inorganic Chemistry

ARTICLE

pubs.acs.org/IC

Multinuclear Cytotoxic Metallodrugs: Physicochemical Characterization and Biological Properties of Novel Heteronuclear Gold−Titanium Complexes

Margot Wenzel,[†] Benoît Bertrand,[†] Marie-Joëlle Eymin,[†] Virginie Comte,[†] Jennifer A. Harvey,[†] Philippe Richard,[†] Michael Groessl,[‡] Olivier Zava,[‡] Hedi Amrouche,[§] Pierre D. Harvey,[§] Pierre Le Gendre,[†] Michel Picquet,*[,†] and Angela Casini*[,‡]

[†]Institut de Chimie Moléculaire de l'Université de Bourgogne, UMR 5260 CNRS - Université de Bourgogne, 9 avenue A. Savary, BP 47870, 21078 Dijon, France

[‡]Institut des Sciences et Ingénierie Chimiques, Ecole Polytechnique Fédérale de Lausanne (EPFL), CH-1015 Lausanne, Switzerland

[§]Département de Chimie, Université de Sherbrooke, Sherbrooke J1K 2R1, Québec, Canada

Supporting Information

ABSTRACT: An unprecedented series of titanocene−gold bi- and trimetallic complexes of the general formula $[[(\eta^5\text{-}C_5H_5)(\mu\text{-}\eta^5{:}\kappa^1\text{-}C_5H_4(CH_2)_nPPh_2)TiCl_2]_mAuCl_x]^{q+}$ (n = 0, 2, or 4; m = 1, x = 1, q = 0 or m = 2, x = 0, q = 1) have been prepared and characterized spectroscopically. The luminescence spectroscopy and photophysics of one of the compounds, $[[(\eta^5\text{-}C_5H_5)(\mu\text{-}\eta^5{:}\kappa^1\text{-}C_5H_4PPh_2)TiCl_2]_2Au]PF_6$, have been investigated in 2MeTHF solution and in the solid state at 77 and 298 K. Evidence for interfragment interactions based on the comparison of electronic band positions and emission lifetimes, namely, triplet energy transfer (ET) from the Au- to the Ti-containing chromophores, is provided. The cytotoxicity of the complexes was evaluated on A2780 ovarian cancer cells and on their cisplatin-resistant cell line A2780cisR; the compounds showed activity in the low micromolar range that was markedly more active than the corresponding titanocene−phosphine precursors $[(\eta^5\text{-}C_5H_5)(\eta^5\text{-}C_5H_4(CH_2)_nPPh_2)TiCl_2]$, cisplatin, and, for some of them, the gold analogue $[(PPh_3)AuCl]$. In an attempt to draw preliminary structure−activity relationships, cell uptake measurements and interaction studies with plasmid DNA and the model protein ubiquitin (Ub) have been undertaken on some of the compounds.

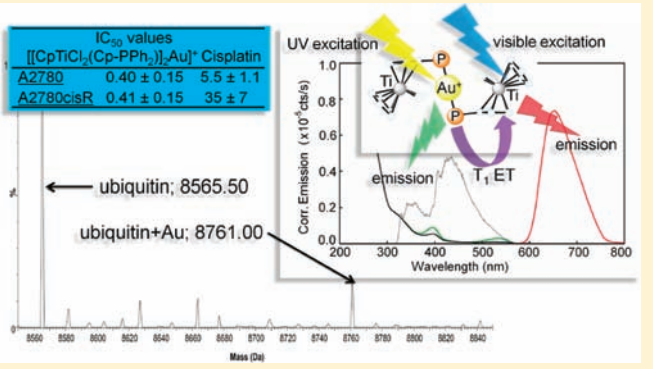

INTRODUCTION

Metal-based drugs are nowadays among the most effective therapeutic agents for the treatment of cancer, with cisplatin, carboplatin, and oxaliplatin being widely used in clinics.[1] However, their effectiveness is still hindered by clinical problems, including acquired or intrinsic resistance, a limited spectrum of activity, and high toxicity leading to side effects.[2] Therefore, anticancer platinum compounds continue to be designed and synthesized through several different approaches in order to improve the therapeutic effects and to overcome the disadvantages of current platinum-based drugs.[3−6] The use of transition metal compounds other than platinum has also attracted attention in metallodrugs' development.[7−9] Among the thousands of inorganic derivatives synthesized and tested so far, only three nonplatinum-based complexes have reached phase II of clinical trials, namely, the organometallic compound titanocene dichloride $(Ti(\eta^5\text{-}C_5H_5)_2Cl_2)$[10] and the Ru-based coordination compounds KP1019[11] and NAMI-A[12] (Chart 1). Recent studies have shown that compounds based on gold are also promising anticancer drugs, and a conspicuous number of gold(III) and gold(I) complexes, with highly different chemical structures, have proven

Chart 1. Nonplatinum-Based Anticancer Complexes Having Reached Phase II of Clinical Trials

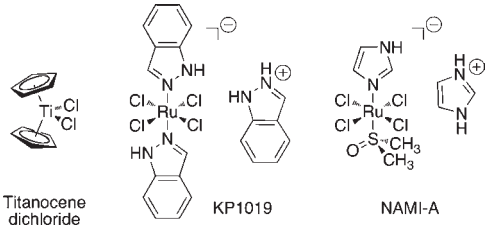

Received: May 30, 2011
Published: August 29, 2011

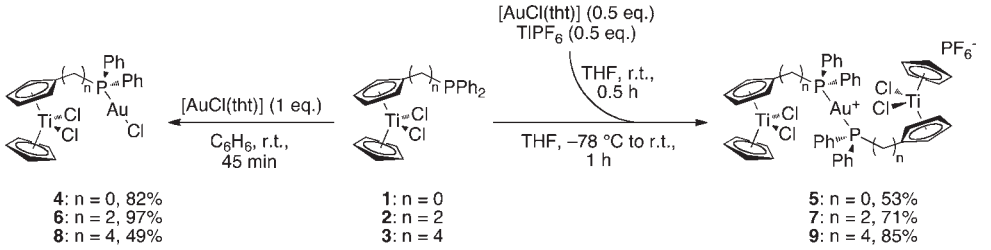

Figure 1. Synthesis of the gold−titanium complexes.

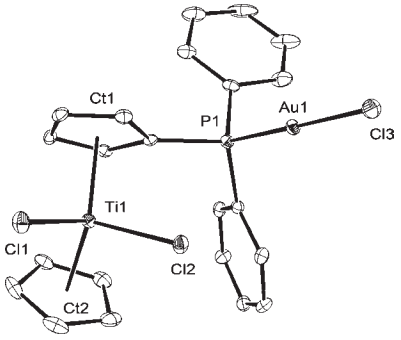

Figure 2. ORTEP representation of **4** at the 50% probability level. For clarity, the H atoms are not shown, and only one molecule is represented. Selected bond distances (Å) and angles (deg) (the second number refers to the second molecule): P1−Au1, 2.227(1), 2.224(1); Au1−Cl3, 2.288(1), 2.285(1); Ti1−Cl1, 2.355(1), 2.352(1); Ti1−Cl2, 2.349(1), 2.347(1); Ti1-Ct1, 2.073(4), 2.078(4); Ti1-Ct2, 2.051(4), 2.052(4); P1−Au1−Cl3, 178.13(4), 175.41(4); Ct1-Ti1-Ct2, 130.72(8), 130.98(8); Cl1−Ti1−Ct2, 92.69(4), 91.43(4).

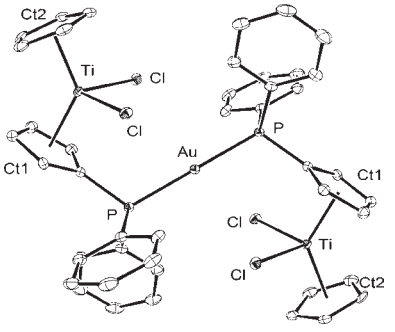

Figure 3. ORTEP representation of **5** at the 50% probability level. For clarity, only one molecule is shown; hydrogen atoms, hexafluorophosphate, and solvates are omitted. Selected bond distances (Å) and angles (deg) (due to the numerous independent molecules in the asymmetric unit, only mean values over equivalent bonds are given): P−Au, 2.309(7); Ti−Cl, 2.349(7); Ti−Ct1, 2.078(7); Ti−Ct2, 2.051(4); Cl−Ti−Cl, 96.4(9); Ct−Ti−Ct, 131.0(8); P−Au−P, 175.7(9) and 180 for the centro symmetric molecules.

to manifest outstanding antiproliferative activities against various human cancer cell lines and in tumor models *in vivo*.[13−16] The pharmacological activities of gold compounds are believed to be caused by selective modification of crucial proteins,[17] and in this context recent mechanistic hypotheses explain their effectiveness via a direct antimitochondrial action,[18] the alteration of the intracellular redox balance through inhibition of thioredoxin reductase,[19] as well as proteasome inhibition.[20]

Indeed, various tactics and some new approaches have been employed to improve the physicochemical and biological properties of metal complexes. Among the possible strategies, the concept of *multinuclearity* has led to innovative chemical and biological properties for a number of bi- and polymetallic complexes, either homo- or heterometallic, as possible anticancer agents. Within this frame, a number of polynuclear platinum, ruthenium, and gold compounds have been developed and biologically characterized.[21−29] Notably, the incorporation of two (or more) metal centers within an extended molecular framework may greatly affect the overall charge of the resulting polynuclear compound, its redox properties, the kinetics of hydrolysis, and its specific reactivity toward biomolecules relative to mononuclear analogues. We have recently characterized a series of bimetallic Ti−Ru complexes based on a titanocene−phosphine backbone anchored to a Ru(II)−arene scaffold, which showed improved antiproliferative effects on cancer cells in comparison to their mononuclear Ti and Ru organometallic precursors.[30] It appears that the enhanced cytotoxic effects might be related to improved stability, solubility, or lipophilicity properties of the compounds induced by the coupling of the two metals.

Following a similar approach, we have synthesized six new binuclear and trinuclear organometallic complexes bearing Au and Ti metals of the type $[[(\eta^5\text{-}C_5H_5)(\mu\text{-}\eta^5{:}\kappa^1\text{-}C_5H_4\text{-}(CH_2)_nPPh_2)TiCl_2]_mAuCl_x]^{q+}$ (n = 0, 2, or 4; m = 1, x = 1, q = 0 or m = 2, x = 0, q = 1; Figure 1, **4**−**9**). The solid state structure of two of these compounds was established by X-ray crystallography, and the luminescence spectroscopic and photophysical properties of $[[(\eta^5\text{-}C_5H_5)(\mu\text{-}\eta^5{:}\kappa^1\text{-}C_5H_4PPh_2)TiCl_2]_2Au]PF_6$ (**5**) have also been investigated. The compounds have been screened for their antiproliferative properties on human ovarian cancer cell lines, and the cellular uptake of two representative members of the series has been evaluated by inductively coupled plasma mass spectrometry (ICP-MS). Complementary studies with model biomolecules have also been performed in order to study the reactivity of the compounds with nucleic acids and proteins.

RESULTS AND DISCUSSION

Synthesis and X-Ray Characterization. Our strategy to construct the gold−titanium complexes consists first of synthesizing the dichlorotitanocenyl−phosphine ligands **1**−**3** and then coordinating the gold metal fragment. In earlier reports, we and others demonstrated the success of this approach in the synthesis of a variety of early late heterobimetallic complexes.[31−34] The organometallic phosphines **1**, **2**, and **3** were prepared according to reported procedures involving the reaction of lithium-(diphenylphosphino)−cyclopentadienide with $CpTiCl_3$ (Cp = η^5-C_5H_5).[35] These phosphines were then treated with one equivalent of [AuCl(tht)] (tht = tetrahydrothiophene) in benzene

dx.doi.org/10.1021/ic201155y |*Inorg. Chem.* 2011, 50, 9472–9480

to afford the neutral bimetallic complexes **4**, **6**, and **8** (Figure 1). The cationic trimetallic complexes **5**, **7**, and **9** have also been prepared from the reaction of **1**−**3** with $[Au(tht)]PF_6$ *in situ* generated as reported in the Experimental Section (Figure 1).

The structures of **4** and **5** were established in the solid state by X-ray crystallography. The asymmetric unit of **4** contains two independent molecules as conformational racemates. Figure 2 shows the molecular structure of one of them, and a selection of bond lengths and angles are listed in the caption (see Supporting Information for crystallographic parameters, Table S1). The titanocene moiety exhibits the usual tetrahedral geometry, with the gold atom pointing away from the open side of the bent metallocene (Ct being the Cp centroid and Clm the midpoint of the two chloride atoms; the P−Ct−Ti−Clm torsion angles are 86.76(7)° and −87.69(6)° in the two conformers). The Au atoms display a linear geometry with P−Au−Cl angles equal to 178.13(4)° and 175.41(4)°. These values correspond well to those found for complexes such as $AuCl(PPh_2CH_2Fc)$ (Fc = ferrocenyl; 176.01(7)°) or $[Au_2Cl_2(\mu\text{-dppf})]$ (dppf = 1,1′- bis-(diphenylphosphino)ferrocene; 179.59(5)°).[36,37] The observed Au−P and Au−Cl distances of 2.227(1) and 2.288(1) Å, respectively (2.224(1) and 2.285(1) Å for the other conformer), are also similar to those of the above-mentioned Au complexes.

In the case of **5**, the asymmetric unit cell contains three PF_6^- anions and three trimetallic cations $[[(\eta^5\text{-}C_5H_5)(\mu\text{-}\eta^5{:}\kappa^1\text{-}C_5H_4PPh_2)TiCl_2]_2Au]^+$, of which two are present as entire molecules, while the third one is present as two half molecules located on symmetry centers. Figure 3 shows one of the cation molecules. All independent molecules are in an antiperiplanar conformation, in which the two organometallic phosphines are oriented in opposite directions. The torsion angles Ct−P−P−Ct are 152.22(7)° and 159.22(8)° for the two molecules, whereas, due to the inversion centers, an ideal value of 180° is observed for the two half molecules. Analogously, the P−Au−P angles are either strictly equal to 180° for the half molecules or to 175.04(4)° and 176.31(4)° for the two entire molecules. Conversely with **4**, the P atoms in **5** are close to the Cl−Ti−Cl bisecting planes: with the same notation as above, the P−Ct−Ti−Clm torsion angles range from 0.5° to 13.8°. All of the other geometrical parameters are comparable for the three trimetallic cations present in the unit cell, only average values are given in the figure caption. The average Au−P distance of 2.309(7) Å is slightly longer than in the neutral bimetallic complex **4**, which seems to be common for gold(I) bis-phosphine complexes.[36]

Photophysical Properties. Compound **5** was further studied for its luminescence properties. In fact, the bent metallocenes of the **IVb** family (Ti, Zr and Hf) are known to exhibit rich photophysical properties.[38] Several theoretical works addressed the electronic structure of such species, and it was quickly established that the nature of the luminescent excited state was a nonlocalized triplet ligand-to-metal charge-transfer (LMCT).[39,40] Subsequently, numerous electrochemical,[41,42] photochemical,[43] and photophysical[40,44−49] studies were reported, including rare examples of luminescence arising from species in solutions.[44,50] The Ph_2P-containing mononuclear complex **1** in 2MeTHF at 77 K exhibits a strong luminescence centered at 659 nm (Figure 4). However, this luminescence is absent at 298 K, which is common to most complexes investigated so far in the literature. The excitation spectrum recorded at 77 K and monitored at 650 nm superimposes the low-energy absorption band at about 400 nm. This band position matches

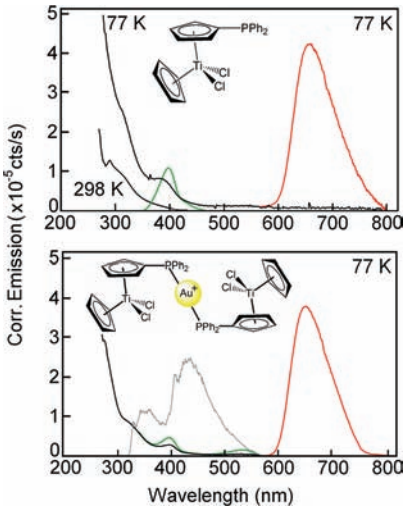

Figure 4. Absorption (black), excitation (green, λ_{exc} = 650 nm, 77 K), and emission spectra (gray, λ_{exc} = 290 nm and red, λ_{exc} = 410 nm, at 77 K) of complexes **1** (up) and **5** (bottom) in 2MeTHF. The relative intensities of the emissions are arbitrary.

Table 1. Emission Data for the $CpTiCl_2(\eta^5\text{-}C_5H_4PPh_2)$ Chromophore in Complexes 1 and 5

	solid state, 77K		2MeTHF, 77 K	
	λ_{max} (nm)	τ_e (μs)	λ_{max} (nm)	τ_e (μs)
$(\eta^5\text{-}C_5H_5)TiCl_2(\eta^5\text{-}C_5H_4PPh_2)$ (**1**)	679	474 ± 10	659	916 ± 3
$[(\eta^5\text{-}C_5H_5)TiCl_2(\mu\text{-}\eta^5{:}\kappa^1\text{-}C_5H_4PPh_2)]_2Au^+$ (**5**)	650	552 ± 6	655	991 ± 6

very well that of the parent compound Cp_2TiCl_2 (666 nm in ethanol/methanol; 77 K).[51] The separation from the lowest energy absorption at ∼400 nm (i.e., for example, at 77 K energy gap = 9800 cm^{-1}) and the long emission lifetime (τ_e = 916 ± 3 μs) indicate that the emission is a phosphorescence. The parent compound Cp_2TiCl_2 exhibits τ_e in the range of 730−800 μs in ethanol/methanol, dichloromethane, and toluene media at 77 K.[45,51] The very strong similarities between these data and those for **1** confirm that the nature of the excited state is the same in both cases (ligand-to-metal excited state; LMCT).[40] In the solid state at 77 K, this strong structureless emission is centered at 679 nm (see Figure S1 in the Supporting Information) and τ_e = 474 ± 22 μs.

The heterotrinuclear complex **5** exhibits similar spectroscopic features associated with the titanocene unit **1** described above, and these are compared in Figure 4 and Table 1. The emission lifetime does not vary significantly, indicating that the nonradiative rate constant, k_{nr}, does not change much upon anchoring the $Au[CpTiCl_2(\eta^5\text{-}C_5H_4PPh_2)]$ pendant group.

Notably, a second emission is detected between 300 and 550 nm for **5** (Figure 4). The nature of this second emission is readily assigned to the Au-containing chromophore based on the reported literature,[52−55] and the titanocene-free $[Ph_3PAuPPh_3]^+$ complex for which the resemblance is striking (Figure 5). The strong emission peak at 485 nm exhibits a long lifetime on the

dx.doi.org/10.1021/ic201155y |*Inorg. Chem.* 2011, 50, 9472–9480

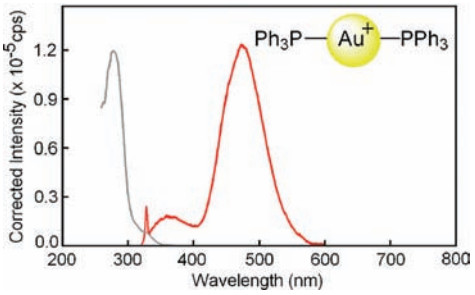

Figure 5. Excitation (gray, λ_{exc} = 480 nm, 77 K) and emission spectra (red, λ_{exc} = 290 nm, 77 K) of $[Ph_3PAuPPh_3]^+$ $(PF_6)^-$ in 2MeTHF.

Table 2. Emission Lifetimes of the Au-Containing Chromophore in Complexes 5 and $[Ph_3PAuPPh_3]^+$

	τ_e (μs)		
	5	$[Ph_3PAuPPh_3]^+$	k_{ET} (s^{-1})
solid state, 77 K	98 ± 1	268 ± 10	3.6×10^5
2MeTHF, 77 K	2.9 ± 1.3	134 ± 10	3.3×10^5

microsecond time scale (Table 2), and the large energy gap between this peak and the shoulder observed in the absorption spectrum at 270 nm recorded in the solid state (Supporting Information; 16 400 cm^{-1}) also indicates that this luminescence arises from a triplet state. It is noteworthy that a comparison of the τ_e data for $[Ph_3PAuPPh_3]^+$ with that of **5** indicates a significative decrease, which means an excited state quenching of the Au-containing chromophore by the $CpTiCl_2(\eta^5\text{-}C_5H_4PPh_2)$ one. An additional emission feature is also depicted at about 360 nm; however, its emission lifetime was too short to be measured on our instrument (i.e., τ_e < 1.5 ns). This emission is very likely fluorescence, as supported by other examples of fluorescence arising from Au-containing species recently reported in the literature.[56,57]

Three types of interactions may be suspected to explain the observed quenching; electron, energy, and atom transfers. The former process can be ruled out because triplet excited states are not prone to electron transfer due to the nature of the excited state (although not excluded for this reason alone), but such transfers at 77 K are most unlikely because of the strong reorganization energy, particularly in the solid state. Moreover, the relatively high negative potential one-electron reduction (−0.82 V vs SCE in CH_2Cl_2) of the Cp_2TiCl_2 residue is accompanied by a loss of Cl^- ions according to electrochemical findings.[42,58] This process requires stabilization of the reduced species, $[Cp_2TiCl]$, by a solvent molecule such as dimethylformamide (DMF) or pyridine (Py), whereas THF is not strong enough for this stabilization.[58] The photoinduced Cl atom transfer, here from Ti to Au, is also ruled out because such a process requires a parallel one-electron transfer process, as recently demonstrated for a similar system, $[CpTiCl_2(C_5H_4PPh_2)]_2Cu^+$,[59] which can be ruled out here. The last process is a triplet energy transfer. Both Ti- and Au-containing units have proven to be involved in triplet energy transfers in the literature. Indeed, the bimolecular triplet energy transfer from various unsaturated hydrocarbons to Cp_2TiCl_2 has been investigated, where the triplet excited state of the Cp_2TiCl_2 complex acts as the acceptor.[48] Similarly, covalently bonded dyads composed of a $PPh_3Au-C\equiv C-$carbazoyl (donor) and fluorine (acceptor) were also investigated for triplet excited state energy transfers.[60] We thus assign the nature of the triplet excited state interactions between the Cp_2TiCl_2 and $[Ph_2PAuPPh_2]^+$ chromophores to energy transfer, the role of donor and acceptor being assigned on the basis of the position of their respective emission depicted in Figure 4.

Hence, the emission lifetimes were analyzed in the context of triplet energy transfers, and their rates, k_{ET}, at 77 K were extracted using eq 1:[61]

$$k_{ET} = \left(\frac{1}{\tau_e} - \frac{1}{\tau_e^0}\right) \quad (1)$$

where τ_e^0 is the emission lifetime for the donor in a structurally related molecule where no energy transfer takes place (here, $[Ph_3PAuPPh_3]^+$), and τ_e is the emission lifetime of the donor in the dyad (here, $-[Ph_2PAuPPh_2]^+-$ in compound **5**). The k_{ET} data are placed in Table 2 and are on the order of 3.5×10^5 s^{-1}, regardless of whether the measurements were performed in the solid state or in 2MeTHF solution at 77 K. The similarity between the measurements indicates that the process is unimolecular, and the measured values suggest a relatively slow through-bond process. Indeed, the molecular geometry of fast through-bond systems ($k_{ET} > 10^6-10^8$ s^{-1}) is linear,[62] whereas here the relative orientation between the Cp_2TiCl_2 and $[Ph_2PAuPPh_2]^+$ chromophores is bent. Therefore, such orientation is most probably not favorable for the requisite good molecular orbital overlap between these two,[63] hence, explaining the slower rate. However, because of this slower rate, total phosphorescence quenching of the donor chromophore does not occur, and the trinuclear complex **5** conveniently exhibits both the blue and the red emissions of the Au- and Ti-containing chromophores, respectively, despite their relative proximity.

Biological Studies. Prior to the biological assays, the solution chemistry of **4**−**7** was analyzed under physiological-type conditions using UV−vis spectrophotometry. The compounds were first dissolved in DMSO and the resulting solutions diluted with phosphate buffered saline (PBS, pH 7.4). Solutions were monitored over 24 h, and representative spectral profiles of **5** are shown in Figure S2 in the Supporting Information. In general, **4**−**7** exhibit intense absorption in the 200−400 nm range, but with time, they exhibit decreases in intensity due to hydrolysis processes. For **4**−**7**, these transitions are maintained over several hours, and therefore the compounds were all considered sufficiently stable for further biological screening. Among the series, **5** was the most stable in solution, even after 6 h of incubation (Figure S2 in the Supporting Information).

The antiproliferative properties of **4**−**7** were assayed by monitoring their ability to inhibit cell growth using the MTT assay (see the Experimental Section). Cytotoxic activity was determined on the human ovarian cancer (A2780) cell line, and its cisplatin-resistant variant (A2780cisR), after 72 h of exposure to the compounds, in comparison to cisplatin. In addition, in order to assess the importance of the various metallo-fragments in determining the observed cytotoxic effects, **8** and **9** were also synthesized and characterized for their antiproliferative properties. The results are summarized in Table 3. Notably, **4**−**9** were almost all more cytotoxic than cisplatin, being active in the low micromolar range on both A2780 and A2780cisR cell lines. Moreover, the most active trinuclear compound **5** was ca. 10-fold more effective than the dinuclear derivative **4**, with IC_{50} ca. 0.40 μM on both cell lines. Interestingly, we could observe that the presence of

dx.doi.org/10.1021/ic201155y |Inorg. Chem. 2011, 50, 9472–9480

Table 3. IC_{50} Values of 1-10 and Cisplatin against Cisplatin-Sensitive (A2780) and -Resistant (A2780cisR) Human Ovarian Carcinoma Cell Lines

	IC_{50} (μM)[a]	
compound	A2780	A2780cisR
1 (η^5-C_5H_5)$TiCl_2$(η^5-$C_5H_4PPh_2$)	53.3 ± 11	62.3 ± 15
2 (η^5-C_5H_5)$TiCl_2$(η^5-$C_5H_4(CH_2)_2PPh_2$)	>50	>50
4 [(η^5-C_5H_5)$TiCl_2$(μ-η^5:κ^1-$C_5H_4PPh_2$)]AuCl	3.7 ± 1.3	3.4 ± 0.9
5 [[(η^5-C_5H_5)$TiCl_2$(μ-η^5:κ^1-$C_5H_4PPh_2$)]$_2$Au]PF_6	0.40 ± 0.15	0.41 ± 0.15
6 [(η^5-C_5H_5)$TiCl_2$(μ-η^5:κ^1-$C_5H_4(CH_2)_2PPh_2$)]AuCl	1.7 ± 0.5	1.6 ± 0.6
7 [[(η^5-C_5H_5)$TiCl_2$(μ-η^5:κ^1-$C_5H_4(CH_2)_2PPh_2$)]$_2$Au]PF_6	4.0 ± 1.2	4.1 ± 0.8
8 [(η^5-C_5H_5)$TiCl_2$(μ-η^5:κ^1-$C_5H_4(CH_2)_4PPh_2$)]AuCl	6.3 ± 2.0	2.8 ± 1.3
9 [[(η^5-C_5H_5)$TiCl_2$(μ-η^5:κ^1-$C_5H_4(CH_2)_4PPh_2$)]$_2$Au]PF_6	4.2 ± 1.3	4.0 ± 1.7
10 (PPh_3)AuCl	2.3 ± 0.7	2.6 ± 0.9
cisplatin	5.5 ± 1.1	35 ± 7

[a] Mean ± SE of at least three determinations.

Table 4. Cell Uptake of 4 and 5 in A2780 and A2780cisR Cancer Cell Lines after Treatment with 1 μM Metal Compound for 24 h

	pmol Au/10^6 cells[a]	
compound	A2780	A2780cisR
4 [(η^5-C_5H_5)$TiCl_2$(μ-η^5:κ^1-$C_5H_4PPh_2$)]AuCl	144 ± 58	256 ± 26
5 [[(η^5-C_5H_5)$TiCl_2$(μ-η^5:κ^1-$C_5H_4PPh_2$)]$_2$Au]PF_6	617 ± 84	820 ± 107

[a] Mean ± SE of at least three determinations.

the alkyl chain in the cationic trinuclear complexes **5**, **7**, and **9** affects their biological properties since the compounds having the longer $(CH_2)_n$ spacer (**7** and **9**) are markedly less effective. It is noteworthy that the mononuclear titanocene precursors **1**−**2** were both poorly cytotoxic (IC_{50} > 50 μM), and only when the gold moiety was linked to the titanium fragment was a significative cytotoxic effect restored, confirming the influence of the Au ion on the pharmacological activity of the compounds. However, the simplest mononuclear Au complex **10** did not reach the same cytotoxic potency of **5**, supporting the hypothesis that multinuclear compounds might have improved chemico-physical properties with respect to their mononuclear precursors. Indeed, **5** showed the highest stability in physiological-type conditions among the series of Au−Ti derivatives, as well as the lowest IC_{50} values.

In order to evaluate the cellular uptake of **5** in comparison to its dinuclear derivative **4**, cell extracts from A2780 and A2780cisR cancer cells treated with a 1 μM metal compound for 24 h at 37 °C were analyzed for their Au content by ICP-MS, as described in the Experimental Section. It must be noted that ICP-MS analysis of Ti in concomitance with Au could not be performed due to different experimental and instrumental requirements in the determinations of the two metal ions. The obtained results expressed as pmol Au/10^6 cells are reported in Table 4. Remarkably, the uptake of **5** is ca. 3−4 times higher than in the case of **4** in each cell line, a fact that may account for the difference in cytotoxic potency between the two compounds.

In order to shed light on the mode of action of the Au−Ti complexes, we investigated their interactions with a few representative biomolecules such as plasmid DNA and ubiquitin (Ub). The reactivity of **5** with pBR322 plasmid DNA was analyzed by gel

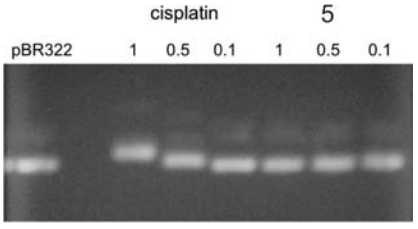

Figure 6. Gel electrophoresis of pBR322 plasmid DNA treated with different concentrations of **5** (r = 1, 0.5, and 0.1; r = metal complex/DNA base pairs) after 24 h incubation in PBS at 37 °C.

electrophoresis according to established procedures, using cisplatin as a reference. Figure 6 shows results for the pBR322 samples treated with increasing amounts of **5** (metal/DNA base pairs = r = 1, 0.5 and 0.1) and incubated in PBS for 24 h at 37 °C. Notably, **5**, contrasting with cisplatin, did not affect the mobility of the supercoiled form of pBR322, even at the highest concentration (r = 1). This observation suggests reduced reactivity with DNA compared to cisplatin, and the nucleic acids are possibly not the only or the primary pharmacological target for this Au−Ti complex, as similarly shown for classical mononuclear gold compounds.[17,64]

Afterward, the binding of **5** to the model protein ubiquitin (Ub) has been evaluated by electrospray ionization mass spectrometry (ESI-MS) following established protocols.[30,65] In a typical experiment, three molar equivalents of **5** were added to an aqueous solution of Ub buffered at pH 7.4 (see the Experimental Section for details). Figure 7 shows the deconvoluted mass spectrum recorded after 1 h incubation for the Ub-**5** sample. In the spectrum, Ub was identified as one of the main peaks at 8565 Da, and a gold-containing species was observed at 8761 Da. This latter peak corresponded to a "naked" Au ion (in which all of the original ligands are absent) bound to Ub. It is noteworthy that the titanium moieties have been released from the original complex, as has been observed for the previously reported dinuclear Ti−Ru complexes,[30] although the influence of the ionization process on fragmentation of the complex cannot be ruled out.

CONCLUSIONS

Novel titanocene−gold bi- and trimetallic complexes have been prepared and characterized. As a representative case,

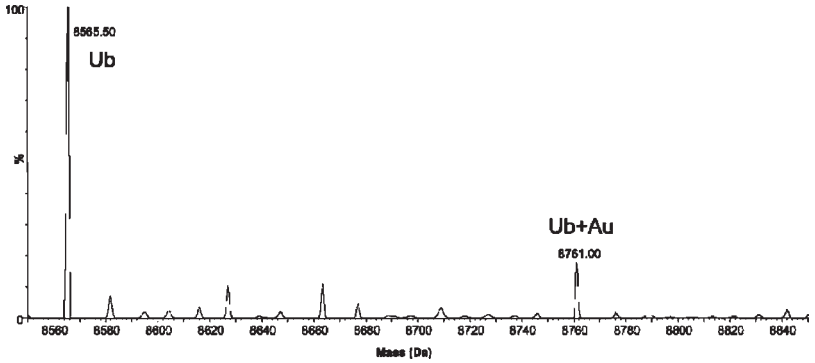

Figure 7. Deconvoluted mass spectrum of Ub incubated with **5** (metal complex/Ub ratio = 3:1) for 24 h at 37 °C.

complex **5** was studied for its photophysical properties. At 77 K, whether in the solid state or in solution, multiple emissions are detected, namely, arising from the LMCT triplet excited state of the $CpTiCl_2(C_5H_4PPh_2)$ chromophore and the Au-containing unit. While the emission lifetime of the $CpTiCl_2(C_5H_4PPh_2)$ chromophore is little affected upon structural modifications, that for the $-[Ph_2PAuPPh_2]^+-$ bridge in compound **5** decreases significantly in comparison with the $[Ph_3PAuPPh_3]^+$ model compound. Arguments were provided to infer the presence of a triplet energy transfer from the $[Ph_2PAuPPh_2]^+$ donor to the titanocene acceptor. The estimated rate for energy transfer is in line with other literature data but also indicates a slow process, which is explained by the poor orbital overlap (Dexter theory) of the two chromophores. This slow rate is convenient because total quenching of the donor phosphorescence (Au−chromophore) does not occur, thus allowing molecular assemblies with multicolor luminescence despite proximity. This property is interesting since **5** can potentially be detected in biological systems, although further studies are necessary to validate this hypothesis.

All compounds were indeed screened for their cytotoxicity against selected cancer cell lines and were found to be considerably more active than their parent mononuclear titanocene−phosphine and even cisplatin, especially in the resistant cell line. Moreover, some of them showed higher activities than the monometallic gold(I) complex $[(PPh_3)AuCl]$, whereas others were revealed to be slightly less active. This effect might be related to modulation of the stability, solubility, or lipophilicity properties of the compounds induced by the titanocene−phosphine moiety. However, other effects may account for the observed cytotoxicity, as illustrated by the difference in cell uptake measurements when performed with the neutral bimetallic complex **4** and its more active cationic trimetallic analogue **5**, in which the same titanocene−phosphine is involved. Finally, complementary investigations performed with the most active complex **5** with respect to its possible interactions with plasmid DNA and ubiquitin (Ub) as representative biomolecules gave insights into its mode of action. Indeed, whereas **5** did not alter the mobility of the supercoiled form of pBR322 plasmid DNA as demonstrated by gel electrophoresis, an ESI-MS study of the same complex incubated over 1 h with the model protein ubiquitin provided evidence for the coordination of a "naked" Au cation to the protein. The latter results together with the cytotoxicity profiles support the idea that the Au center in the bimetallic scaffold plays a fundamental role in determining the biological activity of the reported compounds, possibly due to its known high affinity for binding to amino acid residues in proteins/enzymes. These observations support the hypothesis that this family of heteronuclear potential metallodrugs operates through a pharmacological mechanism in which nucleic acids are not the only or primary target.

EXPERIMENTAL SECTION

Synthesis. *General Remarks.* All reactions were carried out under an atmosphere of purified argon using Schlenk techniques. Solvents were dried and distilled under argon before use. The complexes $[(\eta^5\text{-}C_5H_5)(\eta^5\text{-}C_5H_4PPh_2)TiCl_2]$ (**1**),[35] $[(\eta^5\text{-}C_5H_5)(\eta^5\text{-}C_5H_4(CH_2)_2PPh_2)TiCl_2]$ (**2**),[66] $[(\eta^5\text{-}C_5H_5)(\eta^5\text{-}C_5H_4(CH_2)_4PPh_2)TiCl_2]$ (**3**),[30] and $[(PPh_3)_2Au]^+PF_6^-$[67] and the precursor $[AuCl(tht)]$[68] were synthesized according to literature procedures. All other reagents were commercially available and used as received. All of the analyses were performed at the "Plateforme d'Analyses Chimiques et de Synthèse Moléculaire de l'Université de Bourgogne". The identity and purity (≥95%) of the complexes were unambiguously established using elemental analysis, high-resolution mass spectrometry, and NMR. Elemental analyses were obtained on a Flash EA 1112 CHNS-O Thermo Electron instrument. The exact masses of the synthesized bimetallic complexes were obtained on a Bruker micrOTOF-Q ESI-MS. ^1H (300.13, 500.13, or 600.13 MHz), ^{31}P (121.49, 202.45, or 242.94 MHz), ^{13}C (125.77 or 150.90 MHz), and ^{19}F (470.59 MHz) NMR spectra were recorded on Bruker 300 Avance III, 500 Avance III, or 600 Avance II spectrometers. Chemical shifts are quoted in parts per million (δ) relative to TMS (^1H and ^{13}C), using the residual protonated solvent (^1H) or the deuterated solvent (^{13}C) as an internal standard. Alternatively, 85% H_3PO_4 (^{31}P) and $CFCl_3$ (^{19}F) were used as external standards. Coupling constants are reported in Hertz.

*$[CpTiCl_2(\mu\text{-}\eta^5{:}\kappa^1\text{-}C_5H_4{-}PPh_2)]AuCl$ (**4**).* A 10 mL Schlenk flask was charged under argon with **1** (100 mg, 0.23 mmol) and Au(tht)Cl (73 mg, 0.23 mmol). A total of 8 mL of degassed benzene was added, and the mixture was stirred at room temperature for 45 min, during which time a pink precipitate slowly formed. The solvent was removed by filtration, and the pink residue was dried under vacuum conditions. The crude product was recrystallized from dichloromethane−hexane to give red crystals (142 mg, 82% yield). $^{31}P\{^1H\}^{39}$ NMR (121.49 MHz, $CDCl_3$): δ 23.9 (s, PPh_2). ^1H NMR (300.13 MHz, $CDCl_3$): δ 7.55−7.36 (m, 10H, Ph), 6.78 (m, 2H, C_5H_4), 6.68 (m, 2H, C_5H_4), 6.61 (s, 5H, C_5H_5). $^{13}C\{^1H\}$ NMR (150.90 MHz, CD_2Cl_2): δ 134.4 (d, J_{CP} = 14 Hz, Ph), 132.1 (s, Ph), 129.4 (d, $^1J_{CP}$ = 62 Hz, Ph), 129.1 (d, J_{CP} = 12 Hz, Ph), 126.1 (d, J_{CP} = 9 Hz, C_5H_4), 121.9 (s, C_5H_5), 119.8 (d, J_{CP} = 9 Hz, C_5H_4), 119.4 (d, $^1J_{CP}$ = 65 H, C_5H_4). Anal. Calcd for $C_{22}H_{19}PCl_3TiAu$ (665.56): C, 39.70; H, 2.88; Found: C, 39.70; H, 2.85. ESI-MS (CH_2Cl_2/MeOH, positive mode; *exact mass* for $C_{22}H_{19}PCl_3TiAu$ calcd m/z 663.94349), found: m/z 628.97697 $[M - Cl]^+$. Calcd: m/z 628.97436. UV−vis, (ε(M^{-1} cm^{-1}): 11 900 (at 313), 2690 (at 392), 220 (at 517 nm).

dx.doi.org/10.1021/ic201155y |*Inorg. Chem.* 2011, 50, 9472–9480

[[CpTiCl$_2$(μ-η^5:κ^1-C$_5$H$_4$PPh$_2$)]$_2$Au]PF$_6$ (**5**). A 10 mL Schlenk flask was charged under argon with Au(tht)Cl (37 mg, 0.115 mmol) and TlPF$_6$ (42.5 mg, 0.115 mmol). A total of 2 mL of THF was added, and the mixture was stirred at room temperature for 30 min. AuPF$_6$ generated *in situ* was filtered and added to a solution of **1** (100 mg, 0.23 mmol) in 6 mL of THF at −78 °C. The mixture was stirred and progressively warmed to room temperature over 1 h. The pink precipitate was isolated and recrystallized from dichloromethane−hexane to give red crystals (74 mg, 53% yield). ^{31}P{^{1}H} NMR (242.94 MHz, CD_2Cl_2): δ 34.0 (s, *P*Ph$_2$), −144.4 (hept, $^1J_{PF}$ = 711 Hz, *P*F$_6$). ^{1}H NMR (600.13 MHz, CD_2Cl_2): δ 7.67−7.43 (m, 20H, Ph), 6.70 (m, 4H, C$_5H_4$), 6.62 (m, 4H, C$_5H_4$), 6.47 (s, 10H, C$_5H_5$). ^{13}C{^{1}H} NMR (125.76 MHz, CD_2Cl_2): δ 135.3 (m, Ph), 132.8 (m, Ph), 132.7 (m, Ph), 130.7 (s, *C*$_5$H$_4$), 129.7 (m, Ph), 122.0 (s, *C*$_5$H$_5$), 119.6 (s, *C*$_5$H$_4$), 115.8 (s, *C*$_5$H$_4$). Anal. Calcd for $C_{44}H_{38}Cl_4F_6P_3Ti_2Au$ (1208.21): C, 43.74; H, 3.17. Found: C, 43.25; H, 3.32. UV−vis, (ε(M^{-1} cm^{-1}): 22 200 (at 287), 4160 (at 392), 580 (at 519 nm)). ESI-MS (CH_2Cl_2, positive mode; *exact mass* for $C_{44}H_{38}P_2Cl_4Ti_2Au^+$ ([M − PF$_6$]$^+$ calcd: *m*/*z* 1060.9824), found: *m*/*z* 1060.9781.

[CpTiCl$_2$(μ-η^5:κ^1-C$_5$H$_4$(CH$_2$)$_2$PPh$_2$)]AuCl (**6**). A 10 mL Schlenk flask was charged under argon with **2** (92.4 mg, 0.20 mmol) and Au(tht)Cl (70 mg, 0.20 mmol). A total of 5 mL of degassed benzene was added, and the mixture was stirred at room temperature for 45 min, during which time a salmon pink precipitate formed. The solvent was removed by filtration, and the salmon pink residue was dried under vacuum conditions. The crude product was recrystallized from dichloromethane−hexane to give pink red crystals (134.8 mg, 97% yield). ^{31}P{^{1}H} NMR (202.45 MHz, $CDCl_3$): δ 28.4 (s, *P*Ph$_2$). ^{1}H NMR (500.13 MHz, $CDCl_3$): δ 7.74−7.70 (m, 4H, Ph), 7.54−7.48 (m, 6H, Ph), 6.58 (s, 5H, C$_5H_5$), 6.44 (m, 2H, C$_5H_4$), 6.30 (m, 2H, C$_5H_4$), 3.18 (m, 2H, CH_2), 2.97 (m, 2H, CH_2). ^{13}C{^{1}H} NMR (125.77 MHz, $CDCl_3$): δ 136.0 (d, $^3J_{CP}$ = 15 Hz, *C*$_5$H$_4$), 133.4 (d, $^3J_{CP}$ = 13 Hz, Ph), 132.1 (d, $^4J_{CP}$ = 3 Hz, Ph), 129.3 (d, $^2J_{CP}$ = 11 Hz, Ph), 128.5 (d, $^1J_{CP}$ = 60 Hz, Ph), 123.6 (s, *C*$_5$H$_4$), 119.8 (s, *C*$_5$H$_5$), 113.8 (s, *C*$_5$H$_4$), 27.4 (d, $^1J_{CP}$ = 39 Hz, *C*H$_2$), 26.2 (d, $^2J_{CP}$ = 5 Hz, *C*H$_2$). Anal. Calcd for $C_{24}H_{23}PCl_3TiAu$ (693.61): C, 41.56; H, 3.34. Found: C, 41.07; H, 3.60. ESI-MS (CH_2Cl_2/MeOH, positive mode; *exact mass* for $C_{24}H_{23}PCl_3TiAu$ calcd: *m*/*z* 691.97479), found: *m*/*z* 653.05654 [M − 2Cl + OMe]$^+$. Calcd: *m*/*z* 653.05521.

[[CpTiCl$_2$(μ-η^5:κ^1-C$_5$H$_4$(CH$_2$)$_2$PPh$_2$)]$_2$Au]PF$_6$ (**7**). A 10 mL Schlenk flask was charged under argon with Au(tht)Cl (80 mg, 0.25 mmol) and TlPF$_6$ (92 mg, 0.25 mmol). A total of 4 mL of THF was added, and the mixture was stirred at room temperature for 30 min. AuPF$_6$ generated *in situ* was filtered and added to a solution of **2** (231 mg, 0.50 mmol) in 5 mL of THF at −78 °C. The mixture was stirred and progressively warmed to room temperature over 1 h. As the product did not precipitate, the solvent was removed under vacuum conditions, and the red powder was dried (226 mg, 71% yield). ^{31}P{^{1}H} NMR (202.45 MHz, CD_2Cl_2): δ 30.5 (s, *P*Ph$_2$), −144.3 (hept, $^1J_{PF}$ = 711 Hz, *P*F$_6$). ^{19}F{^{1}H} NMR (470.59 MHz, CD_2Cl_2): δ 72.5 (d, $^1J_{FP}$ = 678 Hz, P*F*$_6$). ^{1}H NMR (500.13 MHz, CD_2Cl_2): δ 7.58−7.44 (m, 20H, Ph), 6.47 (s, 10H, C$_5H_5$), 6.33 (m, 4H, C$_5H_4$), 6.20 (m, 4H, C$_5H_4$), 3.02−2.84 (m, 8H, CH_2). ^{13}C{^{1}H} NMR (125.77 MHz, CD_2Cl_2): δ 138.9 (s, *C*$_5$H$_4$), 137.0 (d, J_{CP} = 18 Hz, Ph), 133.1 (d, J_{CP} = 14 Hz, Ph), 131.8 (s, Ph), 129.8 (d, J_{CP} = 10 Hz, Ph), 123.3 (s, *C*$_5$H$_4$), 120.5 (s, *C*$_5$H$_5$), 114.9 (s, *C*$_5$H$_4$), 27.4 (d, J_{CP} = 23 Hz, *C*H$_2$), 26.7 (d, J_{CP} = 8 Hz, *C*H$_2$). ESI-MS (CH_2Cl_2, positive mode; *exact mass* for $C_{48}H_{46}Cl_4P_2Ti_2Au^+$ [M − PF$_6$]$^+$, calcd: *m*/*z* 1117.04504), found: *m*/*z* 1117.04968.

[CpTiCl$_2$(μ-η^5:κ^1-C$_5$H$_4$(CH$_2$)$_4$PPh$_2$)]AuCl (**8**). A 10 mL Schlenk flask was charged under argon with **3** (61 mg, 0.13 mmol) and Au(tht)Cl (40 mg, 0.13 mmol). A total of 2 mL of degassed benzene was added, and the mixture was stirred at room temperature for 45 min, during which time an orange precipitate partially formed. The solvent was removed by filtration, and the orange residue was dried under vacuum conditions. The crude product was recrystallized from dichloromethane−hexane (45.6 mg, 49% yield). ^{31}P{^{1}H} NMR (202.45 MHz, $CDCl_3$): δ 29.2 (s, *P*Ph$_2$). ^{1}H NMR (500.13 MHz, $CDCl_3$): δ 7.69−7.49 (m, 10H, Ph), 6.58 (s, 5H, C$_5H_5$), 6.45 (m, 2H, C$_5H_4$), 6.33 (m, 2H, C$_5H_4$), 2.77 (t, $^1J_{CP}$ = 7.7 Hz, 2H, CH_2), 2.48 (m, 2H, CH_2), 1.85−1.69 (m, 4H, CH_2). ^{13}C{^{1}H} NMR (125.77 MHz, $CDCl_3$): δ 138.5 (s, *C*$_5$H$_4$), 133.1 (d, $^3J_{CP}$ = 13 Hz, Ph), 132.0 (d, $^4J_{CP}$ = 1 Hz, Ph), 129.4 (d, $^2J_{CP}$ = 11 Hz, Ph), 129.2 (d, $^1J_{CP}$ = 60 Hz, Ph), 122.8 (s, *C*$_5$H$_4$), 119.7 (s, *C*$_5$H$_5$), 115.4 (s, *C*$_5$H$_4$), 30.5 (d, $^2J_{CP}$ = 15 Hz, *C*H$_2$), 30.0 (s, *C*H$_2$), 27.9 (d, $^1J_{CP}$ = 38 Hz, *C*H$_2$), 25.0 (d, $^3J_{CP}$ = 3 Hz, *C*H$_2$). ESI-MS (CH_2Cl_2, positive mode; *exact mass* for $C_{26}H_{27}Cl_3PTiAu$ calcd: *m*/*z* 720.00609), found: *m*/*z* 685.03751 [M − Cl]$^+$. Calcd: *m*/*z* 685.03703.

[[CpTiCl$_2$(μ-η^5:κ^1-C$_5$H$_4$(CH$_2$)$_4$PPh$_2$)]$_2$Au]PF$_6$ (**9**). A 10 mL Schlenk flask was charged under argon with Au(tht)Cl (100 mg, 0.31 mmol) and TlPF$_6$ (115 mg, 0.31 mmol). A total of 4 mL of THF was added, and the mixture was stirred at room temperature for 30 min. AuPF$_6$ generated *in situ* was filtered and added to a solution of **3** (305 mg, 0.62 mmol) in 10 mL of THF at −78 °C. The mixture was stirred and progressively warmed to room temperature over 1 h. As the product did not precipitate, the solvent was removed under vacuum conditions, and the red powder was dried (348 mg, 85% yield). ^{31}P{^{1}H} NMR (202.45 MHz, CD_2Cl_2): δ 40.6 (s, *P*Ph$_2$), −144.3 (hept, $^1J_{PF}$ = 712 Hz, *P*F$_6$). ^{1}H NMR (500.13 MHz, CD_2Cl_2): δ 7.69−7.61 (m, 20H, Ph), 6.56 (s, 10H, C$_5H_5$), 6.44 (m, 4H, C$_5H_4$), 6.27 (m, 4H, C$_5H_4$), 2.77−2.70 (m, 8H, CH_2), 1.85 (m, 4H, CH_2), 1.73 (m, 4H, CH_2). ^{13}C{^{1}H} NMR (125.77 MHz, CD_2Cl_2): δ 138.0 (s, *C*$_5$H$_4$), 133.0 (d, $^3J_{CP}$ = 7.5 Hz, Ph), 132.4 (m, Ph), 129.8 (m, Ph), 128.9 (m, Ph), 123.1 (s, *C*$_5$H$_4$), 119.8 (s, *C*$_5$H$_5$), 115.0 (s, *C*$_5$H$_4$), 31.6 (s, *C*H$_2$), 30.1 (s, *C*H$_2$), 22.6 (s, *C*H$_2$), 22.3 (s, *C*H$_2$). ESI-MS (CH_2Cl_2/MeOH, positive mode; *exact mass* for $C_{52}H_{54}Cl_4P_2Ti_2Au^+$ [M − PF$_6$]$^+$, calcd: *m*/*z* 1173.10765), found: *m*/*z* 1173.11582; 1169.15554 [M − PF$_6$ − Cl + OMe]$^+$. Calcd: *m*/*z* 1169.15826.

X-Ray Diffraction Analysis. Crystals of **4** and **5** were obtained from the slow diffusion of hexane onto a CH_2Cl_2 solution of the compound. Intensity data were collected on a Nonius Kappa CCD at 115 K. The structures were solved by direct methods (SIR92)[69] and refined with full-matrix (for **4**) or full-matrix-block (for **5**) least-squares methods based on F^2 (SHELXL-97)[70] with the aid of the WINGX program.[71] All non-hydrogen atoms were refined with anisotropic thermal parameters. Hydrogen atoms were included in their calculated positions and refined with a riding model. Due to the large number of parameters, **5** was refined by a two-block full-matrix least-squares procedure. In this structure, one of the three PF$_6$ anions and one of the seven dichloromethane solvates was found to be disordered on two positions (occupations: 0.70/0.30 in both cases), and a rigid group refinement was applied for both disordered molecules. Crystallographic data are reported in Table S1 in the Supporting Information.

Photophysical Measurements. The emission and excitation spectra were obtained using a double monochromator Fluorolog 2 instrument from Spex. Phosphorescence time-resolved measurements were performed on a PTI LS-100 using a 1 μs tungsten-flash lamp. Fluorescence and phosphorescence lifetimes were measured on a Timemaster Model TM-3/2003 apparatus from PTI. The source was nitrogen laser with a high-resolution dye laser (fwhm ∼ 1400 ps), and the fluorescence lifetimes were obtained from high-quality decays and deconvolution or distribution lifetimes analysis. The uncertainties were about ±40 ps based on multiple measurements.

UV−Visible Absorption Spectroscopy. The absorption spectra of the compounds in the UV−visible region were recorded on a Jasco V-550 spectrophotometer. The hydrolysis experiments were carried out with solutions of compounds (10^{-4} M) in a PBS buffer (pH 7.4) at 37 °C by monitoring the electronic spectra of the resulting mixtures over 24 h at room temperature.

Cell Culture and Inhibition of Cell Growth. Human A2780 and A2780cisR ovarian carcinoma cell lines were obtained from the European

Centre of Cell Cultures (ECACC, Salisbury, U.K.) and maintained in a culture as described by the provider. The cells were routinely grown in an RPMI 1640 medium containing 10% fetal calf serum (FCS) and antibiotics at 37 °C and 6% CO_2. For evaluation of growth inhibition tests, the cells were seeded in 96-well plates (Costar, Integra Biosciences, Cambridge, MA) and grown for 24 h in a complete medium. Stock solutions of the compounds were prepared by dissolving the compounds in 1 mL of DMSO to reach a concentration of 10^{-2} M. They were then diluted in an RPMI medium and added to the wells (100 μL) to obtain a final concentration ranging between 0 and 80 μM. DMSO at comparable concentrations did not show any effects on cell cytotoxicity. After 72 h of incubation at 37 °C, 20 μL of a solution of MTT (3-(4,5-dimethylthiazol-2-yl)-2,5-diphenyltetrazolium bromide) in PBS (2 mg mL^{-1}) was added to each well, and the plates were then incubated for 2 h at 37 °C. The medium was then aspirated, and DMSO (100 μL) was added to dissolve the precipitate. The absorbance of each well was measured at 580 nm using a 96-well multiwell-plate reader (iEMS Reader MF, Labsystems, Bioconcept, Switzerland) and compared to the values of control cells incubated without complexes. The IC_{50} values for the inhibition of cell growth were determined by fitting the plot of the percentage of surviving cells against the drug concentration using a sigmoidal function (Origin v7.5).

Cell Uptake Studies and ICP-MS Analysis. Human A2780 ovarian carcinoma cells were obtained from the European Centre of Cell Cultures (ECACC, Salisbury, U.K.) and maintained in a culture as described by the provider (RPMI 1640 medium containing 10% fetal calf serum and antibiotics at 37 °C and 5% CO_2). For evaluation of the cell uptake, cells were seeded in six-well plates and grown to approximately 70% confluency and incubated with the corresponding metallodrug at 1 μM for 24 h. At the end of the incubation period, cells were rinsed with 5 mL of PBS, detached by adding 0.4 mL of enzyme free cell dissociation solution (Millipore, Switzerland), and collected by centrifugation. Cell lysis was achieved using a freeze−thaw technique that was recently found to be suitable for cell uptake studies.[72] All samples were analyzed for their protein content (to establish the number of cells per sample) prior to ICP-MS determination using a BCA assay (Sigma Aldrich, Switzerland). All samples were digested in ICP-MS-grade concentrated hydrochloric acid (Sigma Aldrich, Switzerland) for 3 h at room temperature and filled to a total volume of 8 mL with ultrapure water. Indium was added as an internal standard at a concentration of 0.5 ppb. Determinations of total metal contents were achieved on an Elan DRC II ICP-MS instrument (Perkin-Elmer, Switzerland) equipped with a Meinhard nebulizer and a cyclonic spray chamber. The ICP-MS instrument was tuned daily using a solution provided by the manufacturer containing 1 ppb of each Mg, In, Ce, Ba, Pb, and U. External standards were prepared gravimetrically in an identical matrix to that of the samples (with regard to internal standard and hydrochloric acid) with single element standards obtained from CPI International (Amsterdam, The Netherlands).

DNA Electrophoresis. Samples of pBR322 plasmid DNA were prepared by adding the required volume of a freshly prepared solution of metal complexes in Milli-Q water. The concentration of plasmid in the reaction mixture was 75 ng/μL, and the concentration of the complexes was varied to give different metal-to-base pair ratios (r = 1, 0.5, and 0.1). The mobility of the metal-complex-treated pBR322 samples was analyzed by gel electrophoresis on a 0.8% (w/v) agarose gel (Boehringer-Mannheim, Mannheim, Germany) at 90 V/cm at 25 °C for 6 h in Tris-acetate/EDTA buffer. The gel was stained for 30 min in 0.5 g/mL (w/v) ethidium bromide, and the bands were analyzed with a UVP gel scanner.

ESI-MS. Samples were prepared by mixing 100 μM Ub (Sigma, U6253) with an excess of **5** (3:1, metal/protein ratio) in a 20 mM $(NH_4)_2CO_3$ buffer (pH 7.4) and incubated for 1 h at 37 °C. Prior to analysis, samples were extensively ultrafiltered using a Centricon YM-3 filter (Amicon Bioseparations, Millipore Corporation) in order to remove the unbound complex. ESI-MS data were acquired on a Q-Tof Ultima mass spectrometer (Waters) fitted with a standard Z-spray ion source and operated in the positive ionization mode. Experimental parameters were set as follows: capillary voltage, 3.5 kV; source temperature, 80 °C; desolvation temperature, 120 °C; sample cone voltage, 100 V; desolvation gas flow, 400 L/h; acquisition window, 300−2000 m/z in 1 s. The samples were diluted 1:20 in water, and 5 μL was introduced into the mass spectrometer by infusion at a flow rate of 20 μL/min with a solution of $CH_3CN/H_2O/HCOOH$, 50:49.8:0.2 (v:v:v). External calibration was carried out with a solution of phosphoric acid at 0.01%. Data were processed using the MassLynx 4.1 software.

■ ASSOCIATED CONTENT

Supporting Information. UV−visible spectra of **5**, emission spectra of complexes **1** and **5** in the solid state at 77 K, and X-ray crystallographic data for **4** and **5** in CIF format. This material is available free of charge via the Internet at http://pubs.acs.org.

■ AUTHOR INFORMATION

Corresponding Author
*E-mail: angela.casini@epfl.ch, michel.picquet@u-bourgogne.fr.

■ ACKNOWLEDGMENT

The authors thank COST D39 action for stimulating discussions. A.C. thanks the Swiss National Science Foundation (AMBIZIONE project no. PZ00P2-121933) and the Swiss Confederation (Action COST D39 − Accord de recherche − SER project no. C09.0027) for financial support. M.P. thanks the Conseil Régional de Bourgogne (*PARI* and *3MIM* programs), the Ministère de l'Enseignement Supérieur et de la Recherche, and the Centre National de la Recherche Scientifique (CNRS) for financial support. The authors wish to thank the Partenariat Hubert Curien (PHC) franco-suisse "Germaine de Staël" (project no. 2010-01/21760SJ, "Novel bimetallic complexes as highly efficient anticancer agents"). M.G. thanks the Austrian Science Foundation for financial support (Schrödinger Fellowship J2882-N19). P.D.H. thanks NSERC (Natural Sciences and Engineering Research Council of Canada) and CEMOPUS (Centre sur les Matériaux Optiques et Photoniques de l'Université de Sherbrooke) for funding. Dr. F. Chaux and M. M. Soustelle are gratefully acknowledged for HR-MS and elemental analysis, respectively.

■ REFERENCES

(1) Muggia, F.; Farrell, N. *Crit. Rev. Oncol. Hemat.* **2005**, *53*, 1–2.
(2) Rabik, C. A.; Dolan, M. E. *Cancer Treat. Rev.* **2007**, *33*, 9–23.
(3) Aris, S. M.; Farrell, N. P. *Eur. J. Inorg. Chem.* **2009**, 1293–1302.
(4) Perez, J. M.; Fuertes, M. A.; Alonso, C.; Navarro-Ranninger, C. *Crit. Rev. Oncol. Hemat.* **2000**, *35*, 109–120.
(5) Coluccia, M.; Natile, G. *Anti-Cancer Agents Med. Chem.* **2007**, *7*, 111–123.
(6) Hall, M. D.; Dolman, R. C.; Hambley, T. W. *Metal Ions Biol. Syst.* **2004**, *42*, 297–322.
(7) Hartinger, C. G.; Dyson, P. J. *Chem. Soc. Rev.* **2009**, *38*, 391–401.
(8) Casini, A.; Hartinger, C. G.; Nazaroy, A. A.; Dyson, P. J. *Med. Organomet. Chem.* **2010**, *32*, 57–80.
(9) Gianferrara, T.; Bratsos, I.; Alessio, E. *Dalton Trans.* **2009**, *37*, 7588–7598.
(10) Lummen, G.; Sperling, H.; Luboldt, H.; Otto, T.; Rubben, H. *Cancer Chemother. Pharmacol.* **1998**, *42*, 415–417.

(11) Hartinger, C. G.; Jakupec, M. A.; Zorbas-Seifried, S.; Groessl, M.; Egger, A.; Berger, W.; Zorbas, H.; Dyson, P. J.; Keppler, B. K. *Chem. Biodiv.* **2008**, *5*, 2140–2155.
(12) Bergamo, A.; Sava, G. *Dalton Trans.* **2007**, 1267–1272.
(13) Nobili, S.; Mini, E.; Landini, I.; Gabbiani, C.; Casini, A.; Messori, L. *Med. Res. Rev.* **2010**, *30*, 550–580.
(14) Fregona, D.; Ronconi, L.; Aldinucci, D. *Drug Discovery Today* **2009**, *14*, 1075–1076.
(15) Sun, R. W. Y.; Che, C. M. *Coord. Chem. Rev.* **2009**, *253*, 1682–1691.
(16) Ott, I. *Coord. Chem. Rev.* **2009**, *253*, 1670–1681.
(17) Casini, A.; Hartinger, C.; Gabbiani, C.; Mini, E.; Dyson, P. J.; Keppler, B. K.; Messori, L. *J. Inorg. Biochem.* **2008**, *102*, 564–575.
(18) Berners-Price, S. J.; Filipovska, A. *Aust. J. Chem.* **2008**, *61*, 661–668.
(19) Bindoli, A.; Rigobello, M. P.; Scutari, G.; Gabbiani, C.; Casini, A.; Messori, L. *Coord. Chem. Rev.* **2009**, *253*, 1692–1707.
(20) Zhang, X.; Frezza, M.; Milacic, V.; Ronconi, L.; Fan, Y. H.; Bi, C. F.; Fregona, D.; Dou, Q. P. *J. Cell. Biochem.* **2010**, *109*, 162–172.
(21) Farrell, N. *Metal Ions Biol. Syst.* **2004**, *42*, 251–296.
(22) Mendoza-Ferri, M. G.; Hartinger, C. G.; Eichinger, R. E.; Stolyarova, N.; Severin, K.; Jakupec, M. A.; Nazarov, A. A.; Keppler, B. K. *Organometallics* **2008**, *27*, 2405–2407.
(23) Mendoza-Ferri, M. G.; Hartinger, C. G.; Mendoza, M. A.; Groessl, M.; Egger, A. E.; Eichinger, R. E.; Mangrum, J. B.; Farrell, N. P.; Maruszak, M.; Bednarski, P. J.; Klein, F.; Jakupec, M. A.; Nazarov, A. A.; Severin, K.; Keppler, B. K. *J. Med. Chem.* **2009**, *52*, 916–925.
(24) Govender, P.; Antonels, N. C.; Mattsson, J.; Renfrew, A. K.; Dyson, P. J.; Moss, J. R.; Therrien, B.; Smith, G. S. *J. Organomet. Chem.* **2009**, *694*, 3470–3476.
(25) Auzias, M.; Gueniat, J.; Therrien, B.; Suss-Fink, G.; Renfrew, A. K.; Dyson, P. J. *J. Organomet. Chem.* **2009**, *694*, 855–861.
(26) Casini, A.; Cinellu, M. A.; Minghetti, G.; Gabbiani, C.; Coronnello, M.; Mini, E.; Messori, L. *J. Med. Chem.* **2006**, *49*, 5524–5531.
(27) Gabbiani, C.; Casini, A.; Messori, L.; Guerri, A.; Cinellu, M. A.; Minghetti, G.; Corsini, M.; Rosani, C.; Zanello, P.; Arca, M. *Inorg. Chem.* **2008**, *47*, 2368–2379.
(28) Cinellu, M. A.; Maiore, L.; Manassero, M.; Casini, A.; Arca, M.; Fiebig, H. H.; Kelter, G.; Michelucci, E.; Pieraccini, G.; Gabbiani, C.; Messori, L. *ACS Med. Chem. Lett.* **2010**, *1*, 336–339.
(29) Vergara, E.; Cerrada, E.; Casini, A.; Zava, O.; Laguna, M.; Dyson, P. J. *Organometallics* **2010**, *29*, 2596–2603.
(30) Pelletier, F.; Comte, V.; Massard, A.; Wenzel, M.; Toulot, S.; Richard, P.; Picquet, M.; Le Gendre, P.; Zava, O.; Edafe, F.; Casini, A.; Dyson, P. J. *J. Med. Chem.* **2010**, *53*, 6923–6933.
(31) Butenschon, H. *Chem. Rev.* **2000**, *100*, 1527–1564.
(32) Comte, V.; Le Gendre, P.; Richard, P.; Moïse, C. *Organometallics* **2005**, *24*, 1439–1444.
(33) Le Gendre, P.; Picquet, M.; Richard, P.; Moïse, C. *J. Organomet. Chem.* **2002**, *643*, 231–236.
(34) Cornelissen, C.; Erker, G.; Kehr, G.; Frohlich, R. *Organometallics* **2005**, *24*, 214–225.
(35) Le Gendre, P.; Richard, P.; Moïse, C. *J. Organomet. Chem.* **2000**, *605*, 151–156.
(36) Barranco, E. N.; Crespo, O.; Gimeno, M. C.; Laguna, A.; Jones, P. G.; Ahrens, B. *Inorg. Chem.* **2000**, *39*, 680–687.
(37) Canales, F.; Gimeno, M. C.; Jones, P. G.; Laguna, A.; Sarroca, C. *Inorg. Chem.* **1997**, *36*, 5206–5211.
(38) Baldo, M. A.; Thompson, M. E.; Forrest, S. R. *Pure Appl. Chem.* **1999**, *71*, 2095–2106.
(39) Bruce, M. R. M.; Kenter, A.; Tyler, D. R. *J. Am. Chem. Soc.* **1984**, *106*, 639–644.
(40) Patrick, E. L.; Ray, C. J.; Meyer, G. D.; Ortiz, T. P.; Marshall, J. A.; Brozik, J. A.; Summers, M. A.; Kenney, J. W. *J. Am. Chem. Soc.* **2003**, *125*, 5461–5470.
(41) Koch, L.; Fakhr, A.; Mugnier, Y.; Roullier, L.; Moïse, C.; Laviron, E. *J. Organomet. Chem.* **1986**, *314*, C17–C20.
(42) Loukova, G. V. *Chem. Phys. Lett.* **2002**, *353*, 244–252.
(43) Bruce, M. R. M.; Sclafani, A.; Tyler, D. R. *Inorg. Chem.* **1986**, *25*, 2546–2549.
(44) Kunkely, H.; Vogler, A. *Eur. J. Inorg. Chem.* **1998**, 1863–1865.
(45) Loukova, G. V.; Smirnov, V. A. *Chem. Phys. Lett.* **2000**, *329*, 437–442.
(46) Hong, E.; Jang, H.; Kim, Y.; Jeoung, S. C.; Do, Y. *Adv. Mater.* **2001**, *13*, 1094–1096.
(47) Loukova, G. V.; Smirnov, V. A.; Starodubova, S. E. *Dokl. Phys. Chem.* **2005**, *404*, 173–175.
(48) Loukova, G. V.; Starodubova, S. E.; Smirnov, V. A. *J. Phys. Chem. A* **2007**, *111*, 10928–10937.
(49) Endeward, B.; Bernardo, M.; Brant, P.; Thomann, H. *J. Am. Chem. Soc.* **2002**, *124*, 7916–7917.
(50) Loukova, G. V.; Huhn, W.; Vasiliev, V. P.; Smirnov, V. A. *J. Phys. Chem. A* **2007**, *111*, 4117–4121.
(51) Kenney, J. W.; Boone, D. R.; Striplin, D. R.; Chen, Y. H.; Hamar, K. B. *Organometallics* **1993**, *12*, 3671–3676.
(52) King, C.; Wang, J. C.; Khan, M. N. I.; Fackler, J. P. *Inorg. Chem.* **1989**, *28*, 2145–2149.
(53) King, C.; Khan, M. N. I.; Staples, R. J.; Fackler, J. P. *Inorg. Chem.* **1992**, *31*, 3236–3238.
(54) Assefa, Z.; Staples, R. J.; Fackler, J. P. *Inorg. Chem.* **1994**, *33*, 2790–2798.
(55) Sinha, P.; Wilson, A. K.; Omary, M. A. *J. Am. Chem. Soc.* **2005**, *127*, 12488–12489.
(56) Lee, Y. A.; McGarrah, J. E.; Lachicotte, R. J.; Eisenberg, R. *J. Am. Chem. Soc.* **2002**, *124*, 10662–10663.
(57) Guyon, F.; Hameau, A.; Khatyr, A.; Knorr, M.; Amrouche, H.; Fortin, D.; Harvey, P. D.; Strohmann, C.; Ndiaye, A. L.; Huch, V.; Veith, M.; Avarvari, N. *Inorg. Chem.* **2008**, *47*, 7483–7492.
(58) Mugnier, Y.; Moïse, C.; Laviron, E. *J. Organomet. Chem.* **1981**, *204*, 61–66.
(59) Le Gendre, P.; Comte, V.; Ondel-Eymin, M. J.; Moïse, C.; Pousson, E.; Richard, P.; Mugnier, Y.; Fortin, D.; Boere, R. T.; Harvey, P. D. *Inorg. Chem.* **2009**, *48*, 3095–3103.
(60) Aly, S. M.; Ho, C. L.; Wong, W. Y.; Fortin, D.; Harvey, P. D. *Macromolecules* **2009**, *42*, 6902–6916.
(61) Faure, S.; Stern, C.; Espinosa, E.; Douville, J.; Guilard, R.; Harvey, P. D. *Chem. Eur. J.* **2005**, *11*, 3469–3481.
(62) Bellows, D.; Goudreault, T.; Aly, S. M.; Fortin, D.; Gros, C. P.; Barbe, J. M.; Harvey, P. D. *Organometallics* **2010**, *29*, 317–325.
(63) Dexter, D. L. *J. Chem. Phys.* **1953**, *21*, 836–850.
(64) Vergara, E.; Casini, A.; Sorrentino, F.; Zava, O.; Cerrada, E.; Rigobello, M. P.; Bindoli, A.; Laguna, M.; Dyson, P. J. *ChemMedChem* **2010**, *5*, 96–102.
(65) Casini, A.; Diawara, M. C.; Scopelliti, R.; Zakeeruddin, S. M.; Grätzel, M.; Dyson, P. J. *Dalton Trans.* **2010**, *39*, 2239–2245.
(66) Leblanc, J. C.; Moïse, C.; Maisonnat, A.; Poilblanc, R.; Charrier, C.; Mathey, F. *J. Organomet. Chem.* **1982**, *231*, C43–C48.
(67) Sykes, A. G.; Mann, K. R. *J. Am. Chem. Soc.* **1990**, *112*, 7247–7254.
(68) Uson, R.; Laguna, A.; Laguna, M.; Briggs, D. A.; Murray, H. H.; Fackler, J. J. P. *Inorg. Synth.* **1989**, *26*, 85–91.
(69) Altomare, A.; Burla, M. C.; Camalli, M.; Cascarano, G. L.; Giacovazzo, C.; Guagliardi, A.; Moliterni, A. G. G.; Polidori, G.; Spagna, R. *J. Appl. Crystallogr.* **1999**, *32*, 115–119.
(70) Sheldrick, G. M. *SHELX97* (Includes SHELXS97 and SHELXL97); Institüt für Anorganische Chemie, University of Göttingen: Göttingen, Germany, 1998.
(71) Farrugia, L. J. *J. Appl. Crystallogr.* **1999**, *32*, 837–838.
(72) Tran, M. Q. T.; Nygren, Y.; Lundin, C.; Naredi, P.; Bjorn, E. *Anal. Biochem.* **2010**, *396*, 76–82.